



Article

Characterization in Potent Modulation on Voltage-Gated Na⁺ Current Exerted by Deltamethrin, a Pyrethroid Insecticide

Mao-Hsun Lin ^{1,†}, Jen-Feng Lin ^{2,†}, Meng-Cheng Yu ³, Sheng-Nan Wu ^{3,4,5,*} , Chao-Liang Wu ⁶ 
and Hsin-Yen Cho ³

¹ Division of Neurology, Department of Internal Medicine, Ditmanson Medical Foundation Chiayi Christian Hospital, Chiayi City 600, Taiwan

² Department of Emergency Medicine, Ditmanson Medical Foundation Chiayi Christian Hospital, Chiayi City 600, Taiwan

³ Department of Physiology, National Cheng Kung University Medical College, Tainan 701, Taiwan

⁴ Institute of Basic Medical Sciences, National Cheng Kung University Medical College, Tainan 701, Taiwan

⁵ Department of Post-Baccalaureate Medicine, National Sun Yat-Sen University, Kaohsiung 804, Taiwan

⁶ Ditmanson Medical Foundation Chiayi Christian Hospital, Chiayi City 600, Taiwan

* Correspondence: snwu@mail.ncku.edu.tw; Tel.: +886-6-2353535-5334; Fax: 886-6-2362780

† These authors contributed equally to this work.



Citation: Lin, M.-H.; Lin, J.-F.; Yu, M.-C.; Wu, S.-N.; Wu, C.-L.; Cho, H.-Y. Characterization in Potent Modulation on Voltage-Gated Na⁺ Current Exerted by Deltamethrin, a Pyrethroid Insecticide. *Int. J. Mol. Sci.* **2022**, *23*, 14733. <https://doi.org/10.3390/ijms232314733>

Academic Editors: José Manuel González Ros and Hiroki Toyoda

Received: 7 October 2022

Accepted: 23 November 2022

Published: 25 November 2022

Publisher's Note: MDPI stays neutral with regard to jurisdictional claims in published maps and institutional affiliations.



Copyright: © 2022 by the authors. Licensee MDPI, Basel, Switzerland. This article is an open access article distributed under the terms and conditions of the Creative Commons Attribution (CC BY) license (<https://creativecommons.org/licenses/by/4.0/>).

Abstract: Deltamethrin (DLT) is a type-II pyrethroid ester insecticide used in agricultural and domestic applications as well as in public health. However, transmembrane ionic channels perturbed by this compound remain largely unclear, although the agent is thought to alter the gating characteristics of voltage-gated Na⁺ (Na_V) channel current. In this study, we reappraised whether and how it and other related compounds can make any further modifications on voltage-gated Na⁺ current (*I*_{Na}) in pituitary tumor (GH₃) cells. Cell exposure to DLT produced a differential and dose-dependent stimulation of peak (transient, *I*_{Na(T)}) or sustained (late, *I*_{Na(L)}) *I*_{Na}; consequently, the EC₅₀ value required for DLT-stimulated *I*_{Na(T)} or *I*_{Na(L)} was determined to be 11.2 or 2.5 μM, respectively. However, neither the fast nor slow component in the inactivation time constant of *I*_{Na(T)} activated by short depolarizing pulse was changed with the DLT presence; conversely, tefluthrin (Tef), a type-I pyrethroid insecticide, can accentuate *I*_{Na} with a slowing in inactivation time course of the current. The *I*_{Na(L)} augmented by DLT was attenuated by further application of either dapagliflozin (Dapa) or amiloride, but not by chlorotoxin. During pulse train (PT) stimulation, with the Tef or DLT presence, the cumulative inhibition of *I*_{Na(T)} became slowed; moreover, following PT stimuli, a large tail current with a slowly recovering process was observed. Alternatively, during rapid depolarizing pulse, the amplitude of *I*_{Na(L)} and tail *I*_{Na} (*I*_{Na(Tail)}) for each depolarizing pulse became progressively increased by adding DLT, not by Tef. The recovery time constant following PT stimulation with continued presence of Tef or DLT was shortened by further addition of Dapa. The voltage-dependent hysteresis (Hys_V) of persistent *I*_{Na} was differentially augmented by Tef or DLT. Taken together, the magnitude, gating, frequency dependence, as well as Hys_V behavior of *I*_{Na} exerted by the presence of DLT or Tef might exert a synergistic impact on varying functional activities of excitable cells in culture or in vivo.

Keywords: pyrethroids; voltage-gated Na⁺ current; late Na⁺ current; transient Na⁺ current; persistent Na⁺ current

1. Introduction

Deltamethrin (DLT, decamethrin) is a cyclopropanecarboxylate ester obtained by formal condensation between 3-(2,2-dibromovinyl)-2,2-dimethylcyclopanecarboxylic acid and cyano(3-phenoxyphenyl)methanol [1,2]. It is viewed to be the active insecticide of the proinsecticide tralomethrin [3–5]. Pyrethroids like DLT or tefluthrin (Tef) have been demonstrated to modify the gating characteristics of voltage-gated Na⁺ (Na_V) channels [6–10].

Deltamethrin (DLT), a neurotoxic type-II pyrethroid ester insecticide [3–5], has been demonstrated previously to cause a reversible sequence of motor symptoms in rats involving hind limb rigidity and choreoathetosis [2,11–13]. Alternatively, DLT was also reported to decrease Cl^- currents through voltage-dependent Cl^- channels and this action probably contributes the most to the features of poisoning with DLT or other type II pyrethroids [14–16]. At relatively high concentrations, pyrethroids can also act on GABA-gated Cl^- channels, which may be responsible for the seizures seen with severe type-II poisoning [2,17].

It has been established that nine isoforms (i.e., $\text{Na}_V1.1$ – 1.9 [or SCN1A – SCN5A and SCN8A – SCN11A]) of the voltage-gated Na^+ (Na_V) channels are widely distributed in mammalian excitable tissues, which include the central or peripheral nervous system, and the endocrine or neuroendocrine system [18–20]. The eukaryotic versions of these Na_V -channel proteins are comprised of a single subunit which contains four six-transmembrane pseudodomains [20,21]. Upon rapid depolarization, the Na_V channels, by which macroscopic voltage-gated Na^+ currents (I_{Na}) are encoded, are characterized by going through rapid transitions from the closed (resting) state to the open state, and then by swiftly changing to the inactivated state [20,21]. The inactivation of I_{Na} has been also demonstrated to accumulate before being stimulated during repetitive short depolarizing pulses [22–25]. Consequently, once being evoked, the increased magnitude of I_{Na} can quickly depolarize the cell membrane through positive feedback cycle and, in turn, elicit the upstroke of the action potentials, thereby intrinsically governing the amplitude, frequency, and/or pattern of firing action potentials, as well as hormonal secretion, in an array of excitable cells [20,21,26,27]. On the other hand, the aberrant changes in Na_V (i.e., $\text{Na}_V1.2$) channel activity occurring in corticostriatal circuits of adult mice were also reported to elevate neuronal excitability [28].

Like the action of tefluthrin (Tef) [7,8,16,26,29], deltamethrin (DLT) was used to kill a wide range of insects [2,6,30]. There is a growing concern over human or animal poisoning as aberrant use in these esters. However, whether and how deltamethrin (DLT) or other structurally similar pyrethroids (e.g., Tef) is able to modify the magnitude, gating kinetics, frequency dependence, and/or voltage-dependent hysteresis ($\text{Hys}_{(V)}$) of I_{Na} remains mostly obscure, although they are recognized to augment the I_{Na} magnitude [6–9].

In light of the aforementioned considerations, we wanted to extensively explore the electrophysiological effects of DLT and other related compounds (e.g., Tef) in pituitary GH_3 sommatolactotrophs with either a single voltage-clamp pulse or pulse train (PT) stimulation. The tetrodotoxin (TTX)-sensitive I_{Na} , which is responsible for the generation of action potentials, has been identified in pituitary tumor (GH_3) cells [18]. The GH_3 cell line has been demonstrated previously to express the α -subunits of $\text{Na}_V1.1$, $\text{Na}_V1.2$, $\text{Na}_V1.3$, and $\text{Na}_V1.6$, as well as the $\beta 1$ and $\beta 3$ -subunits of Na_V channel [18,31]. In the current investigations, we intended to (1) evaluate if DLT has any perturbations on the peak (transient, $I_{\text{Na}(T)}$) and sustained (late, $I_{\text{Na}(L)}$) components of I_{Na} intrinsically in these cells; (2) examine if this compound affects either magnitude or time course of I_{Na} during as well as following 1-s pulse train (PT) stimulation; (3) explore whether or not the $\text{Hys}_{(V)}$'s behavior of persistent I_{Na} ($I_{\text{Na}(P)}$) could be seriously disturbed by the presence of DLT; and (4) the molecular docking between the DLT molecule and the $\text{hNa}_V1.5$ channel was also predicted. The present results disclosed that the differential and dose-dependent stimulation of $I_{\text{Na}(T)}$ and $I_{\text{Na}(L)}$ by DLT as well as its perturbations either on I_{Na} occurring during or following PT stimulation, or on $\text{Hys}_{(V)}$ properties of $I_{\text{Na}(P)}$ may potentially converge to engage in a great impact on electrical behaviors of mammalian excitable cells (e.g., GH_3 cells).

2. Results

2.1. Modification by Deltamethrin (DLT) or Tefluthrin (Tef) on Voltage-Gated Na^+ Current (I_{Na}) Measured from Pituitary GH_3 Cells

In the first stage of whole-cell current recordings, we measured the effects of DLT or Tef on the magnitude and inactivation time course of I_{Na} activated in response to

abrupt depolarizing pulse. We placed cells in Ca^{2+} -free, Tyrode's solution containing 10 mM tetraethylammonium chloride (TEA), and the pipette used was filled up with a Cs^{+} -containing solution. As demonstrated in Figure 1A, two minutes after cells were continually exposed to DLT or Tef at a concentration of 10 μM , the amplitude in the transient ($I_{\text{Na(T)}}$) or late ($I_{\text{Na(L)}}$) component of I_{Na} activated by 20-ms depolarizing pulse from -80 to -10 mV was progressively raised. For example, as the rectangular voltage step from -80 to -10 mV with a duration of 20 ms was given (indicated in the uppermost part of Figure 1A) to activate I_{Na} , the addition of 10 μM DLT was found to result in a striking increase in either $I_{\text{Na(T)}}$ or $I_{\text{Na(L)}}$ amplitude to 512 ± 17 pA ($n = 9, p < 0.05$) or 128 ± 9 pA ($n = 9, p < 0.05$) from control values of 401 ± 15 or 22 ± 5 pA ($n = 9$), respectively. After washout of DLT, $I_{\text{Na(T)}}$ or $I_{\text{Na(L)}}$ was returned to 409 ± 17 or 28 ± 7 pA ($n = 9$). Likewise, the presence of 10 μM Tef also measurably increased $I_{\text{Na(T)}}$ or $I_{\text{Na(L)}}$ amplitude from 409 ± 14 pA ($n = 9$) or 32 ± 6 pA ($n = 9$) to 499 ± 16 pA ($n = 9, p < 0.05$) or 162 ± 11 pA ($n = 9, p < 0.05$), respectively. However, with cell exposure to 10 μM DLT, neither fast nor slow time constant of $I_{\text{Na(T)}}$ inactivation in response to rapid membrane depolarization was evidently changed. Alternatively, with the presence of 10 μM Tef, the slow component in the time constant of $I_{\text{Na(T)}}$ inactivation was strikingly raised to 19 ± 2 msec ($n = 9, p < 0.05$) from a control value of 0.9 ± 0.2 msec ($n = 9$). The time course of effects of DLT (10 μM) on the amplitude of $I_{\text{Na(Tot)}}$, $I_{\text{Na(L)}}$ or $I_{\text{Na(T)}}$ is illustrated in Figure 1B. Of note, during exposure to 10 mM DLT, the amplitude of $I_{\text{Na(Tot)}}$, $I_{\text{Na(L)}}$, or $I_{\text{Na(T)}}$ was increased to 177 ± 21 % ($n = 8$), 1752 ± 105 % (i.e., around 1.7-fold) ($n = 8$), or 24 ± 6 % ($n = 8$), respectively.

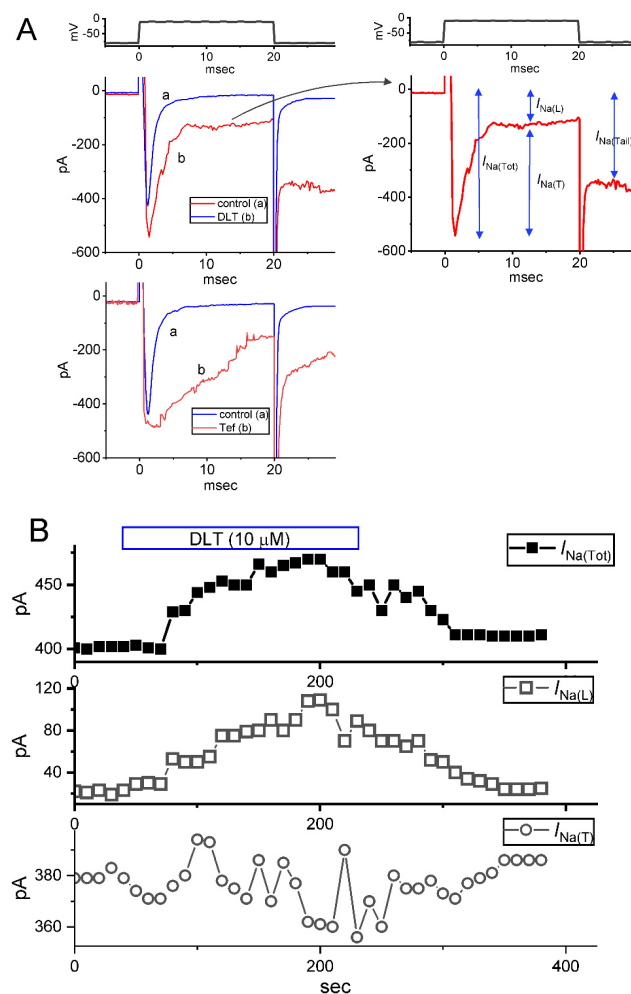


Figure 1. Cont.

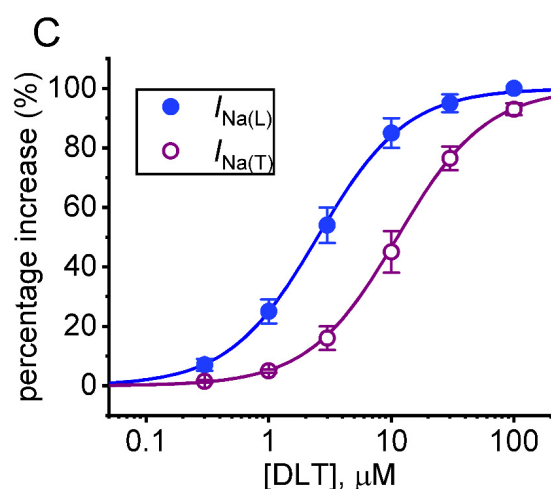


Figure 1. Effect of deltamethrin (DLT) or tefluthrin (Tef) on voltage-gated Na^+ current (I_{Na}) measured from pituitary GH_3 lactotrophs. This set of experiments was made in cells placed in Ca^{2+} -free, Tyrode's solution containing 10 mM tetraethylammonium chloride (TEA), and the measuring electrode was filled with an internal solution enriched with Cs^+ . (A) Exemplar current traces obtained in (a, blue color) the control conditions (i.e., neither DLT nor Tef was present) and during cell exposure to either 10 μM DLT (b, upper, red color) or 10 μM Tef (b, lower, red color). The voltage-clamp protocol is illustrated atop recorded current traces. The graph shown in the right side of (A) denotes the expanded record from the observed current trace (red color) in the presence of 10 μM DLT and the definition of transient Na^+ current ($I_{\text{Na(T)}}$), late Na^+ current ($I_{\text{Na(L)}}$), total Na^+ current ($I_{\text{Na(Tot)}}$), or tail Na^+ current ($I_{\text{Na(Tail)}}$) is marked (indicated with blue double arrows). (B) Time course of effects of 10 μM DLT on the amplitude of $I_{\text{Na(Tot)}}$ (upper), $I_{\text{Na(L)}}$ (middle), and $I_{\text{Na(T)}}$ (lower). Each point was taken at a rate of 0.1 Hz. The horizontal bar shown above indicated the application of DLT. (C) Concentration-dependent relationship of DLT on $I_{\text{Na(T)}}$ (purple open circles) or $I_{\text{Na(L)}}$ (blue solid circles) activated by short depolarizing step. Each data point in this graph represents mean \pm SEM of 9 cells. According to the averaged data, the smooth line represents the best fit to the Hill equation as described in Materials and Methods.

Figure 1C demonstrates that the addition of DLT to the bath can concentration-dependently increase the amplitude of $I_{\text{Na(T)}}$ or $I_{\text{Na(L)}}$ activated by short depolarizing step. According to the Hill equation stated under Materials and Methods, the EC_{50} value needed for DLT-stimulated $I_{\text{Na(T)}}$ or $I_{\text{Na(L)}}$ observed in GH_3 cells was calculated as 11.2 or 2.5 μM , respectively. Consistent with previous studies [6,8], the experimental observations, therefore, enable us to reflect that the DLT presence exerts a stimulatory action on the magnitude of $I_{\text{Na(T)}}$ and $I_{\text{Na(L)}}$ natively expressed in GH_3 cells, and that this compound tends to be selective for $I_{\text{Na(L)}}$ over $I_{\text{Na(T)}}$ during rectangular depolarizing pulse.

2.2. Comparison among Effects of Tef, DLT, Tef plus Chlorotoxin (ChloroTx), DLT plus ChloroTx, Tef plus Dapaglifozin (Dapa), DLT plus Dapa, and DLT plus Amiloride on $I_{\text{Na(L)}}$ Amplitude Measured from GH_3 Cells

Exposure to pyrethroids (e.g., DLT) has been previously demonstrated to activate Cl^- currents [14–16]. We further compared the effects of Tef, DLT or their combinations with ChloroTx, Dapa, or amiloride on $I_{\text{Na(L)}}$ amplitude. ChloroTx was reported to suppress Cl^- current, Dapa was an inhibitor of $I_{\text{Na(L)}}$ [32,33], and amiloride can attenuate the pyrethroids-stimulated sodium transport [16]. As summarized in Figure 2, with continued presence of Tef or DLT, the further exposure to ChloroTx (1 μM) failed to modify their stimulation of $I_{\text{Na(L)}}$. Dapa (10 mM) or amiloride (10 mM) alone decrease the $I_{\text{Na(L)}}$ amplitude to 31 ± 2 pA ($n = 8$, $p < 0.05$) or 28 ± 2 pA ($n = 8$, $p < 0.05$) from control value of 50.3 ± 3 pA ($n = 8$). Moreover, the subsequent presence of either Dapa (10 μM) or amiloride (10 μM) was able to attenuate Tef- or DLT-mediated increase of $I_{\text{Na(L)}}$ effectively. The results prompted us

to suggest that either Dapa or amiloride could directly cause an inhibitory effect on the amplitude of $I_{Na(L)}$ observed in GH₃ cells [32,33].

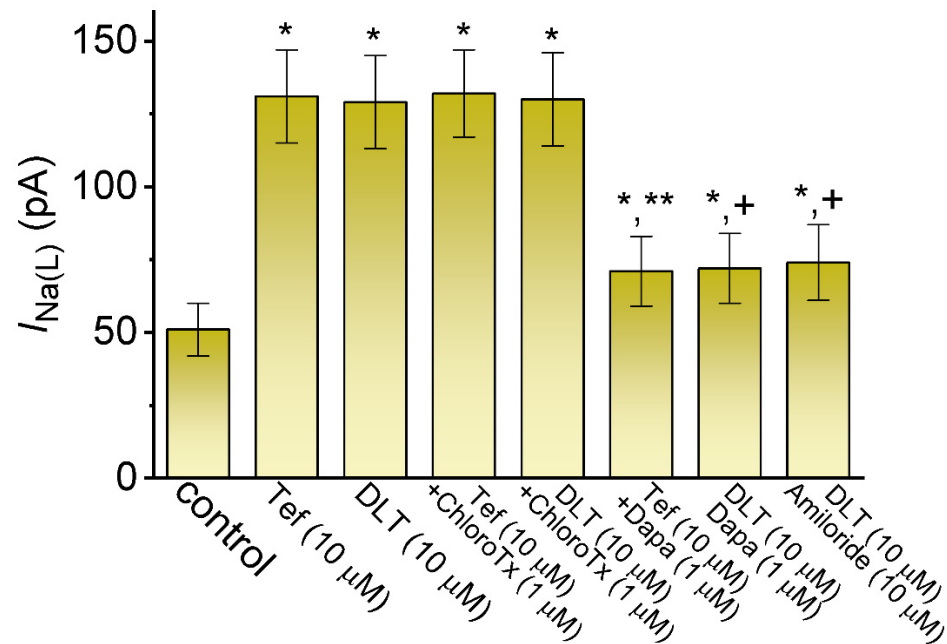


Figure 2. Comparison among effects of Tef, DLT, Tef plus chlorotoxin (ChloroTx), DLT plus ChloroTx, Tef plus dapagliflozin (Dapa), DLT plus Dapa, and DLT plus amiloride on the amplitude of $I_{Na(L)}$ measured from GH₃ cells. The I_{Na} was elicited by 20 ms depolarizing voltage command from -80 to -10 mV for a duration of 20 ms at a rate of 0.2 Hz. The $I_{Na(L)}$ amplitudes during exposure to different tested compounds were measured at the end of each depolarizing step. Each bar represents the mean \pm SEM ($n = 8$). * Significantly different from control ($p < 0.05$), ** significantly different from Tef (10 μ M) alone group ($p < 0.05$), and + significant different from DLT (10 μ M) alone group ($p < 0.05$).

2.3. Effect of DLT on Mean Current Versus Voltage (I - V) Relationship of $I_{Na(T)}$ and $I_{Na(L)}$

We next explored any perturbations of this compound on the amplitude of $I_{Na(T)}$ or $I_{Na(L)}$ measured from the different level of membrane potentials. As demonstrated in Figure 3A,B, a steady-state I - V relationship of $I_{Na(T)}$ and $I_{Na(L)}$ acquired with or without the DLT (10 μ M) presence was established in these cells. The appearance of 10 μ M DLT resulted in a striking increase in the $I_{Na(T)}$ or $I_{Na(L)}$ amplitude elicited by abrupt depolarizing steps. For example, when the tested cells were rapidly depolarized from -80 to -10 mV, the addition of 10 μ M DLT raised either $I_{Na(T)}$ or $I_{Na(L)}$ magnitude from 729 ± 54 to 952 ± 76 pA ($n = 8$, $p < 0.05$), or from 26 ± 34 to 265 ± 48 pA ($n = 8$, $p < 0.05$), respectively. However, the steady-state I - V relationship of $I_{Na(T)}$ or $I_{Na(L)}$ remained unaffected during exposure to 10 μ M DLT, despite a marked increase in $I_{Na(T)}$ or $I_{Na(L)}$ magnitude. The relationship (i.e., G - V relationship) for the conductance of $I_{Na(T)}$ or $I_{Na(L)}$ with or without the application of 10 μ M DLT was also established and depicted in Figure 3C. The $V_{1/2}$ value for G - V relationship of $I_{Na(T)}$ or $I_{Na(L)}$ between the absence and presence of 10 mM DLT did not differ significantly $\{(-19.9 \pm 1.8$ mV [control] versus -20.5 ± 1.7 mV [in the presence of DLT]; $n = 8$, $p > 0.05$, for the results of $I_{Na(T)}$), or $(-18.4 \pm 1.6$ mV [control] versus -18.5 ± 1.6 mV [in the presence of DLT]; $n = 8$, $p > 0.05$, for the results of $I_{Na(L)})$.

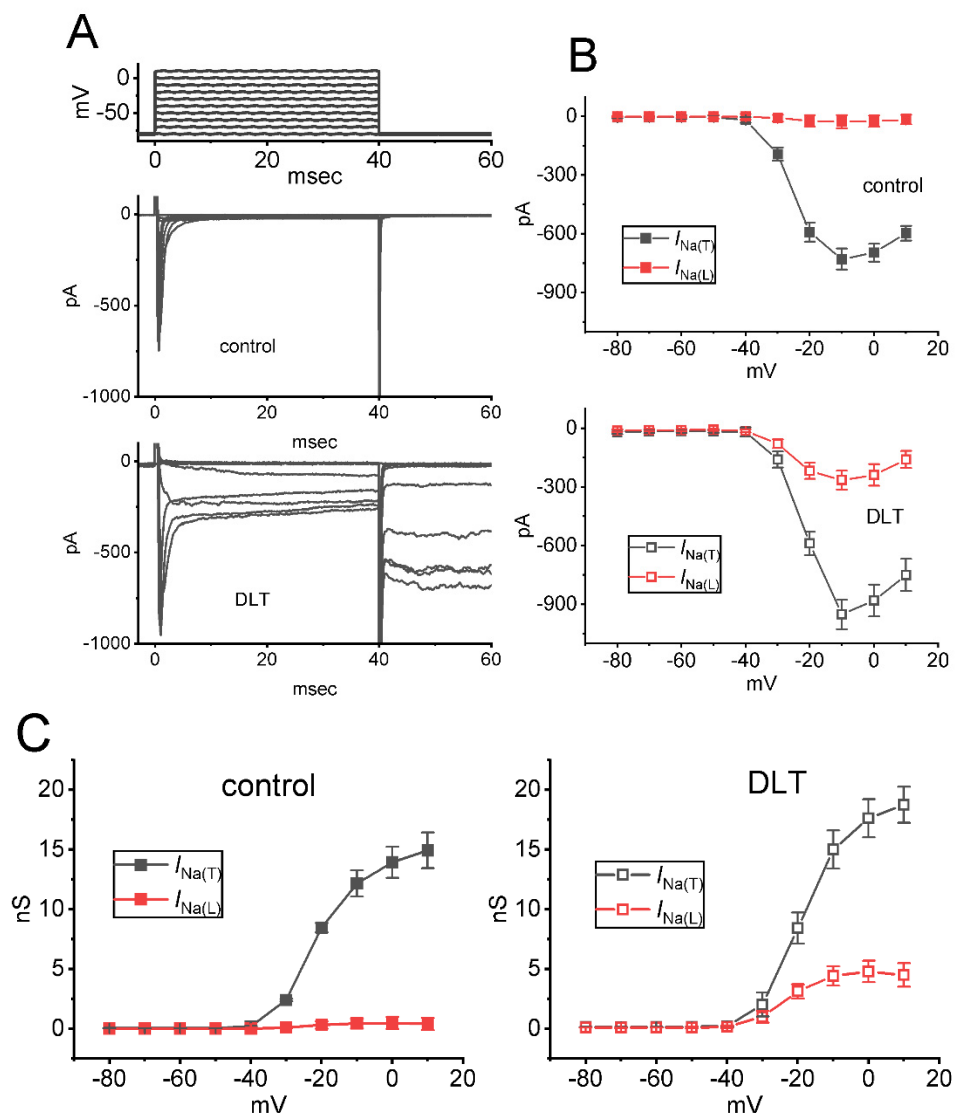


Figure 3. Effect of DLT on the steady-state current versus voltage (I-V) relationship of $I_{Na(T)}$ and $I_{Na(L)}$ identified from GH₃ cells. In this set of experiments, we held each cell at -80 mV, and varying depolarizing command voltages from -80 to $+10$ mV in 10 -mV steps were delivered to evoke $I_{Na(T)}$ and $I_{Na(L)}$. **(A)** Exemplar current traces obtained either in the control condition (upper) or with the presence of 10 μ M DLT (lower). The uppermost part is the voltage-clamp protocol given. **(B)** The mean I-V relationship of $I_{Na(T)}$ (black symbols) or $I_{Na(L)}$ (red symbols) in control (upper, solid symbols) and during exposure to 10 μ M DLT (lower, open symbols) (mean \pm SEM; $n = 8$ for each point). Either $I_{Na(T)}$ or $I_{Na(L)}$ was measured at the beginning or end of each depolarizing pulse. **(C)** Conductance versus voltage relationship of $I_{Na(T)}$ (black symbols) or $I_{Na(L)}$ (red symbols) in the control period (left side) and during cell exposure to 10 μ M DLT (right side) (mean \pm SEM; $n = 8$ for each point).

2.4. Tef- or DLT-Mediated Slowing in Cumulative Inhibition of $I_{Na(T)}$ during Rapid Depolarizing Stimuli

It has been demonstrated that, prior to being activated during repetitive short pulses, the inactivation of $I_{Na(T)}$ is able to accumulate [22,23,25,34–36]. For this reason, we next explored if Tef or DLT could modify the extent of $I_{Na(T)}$ activated either during or following the PT depolarizing stimuli. In this set of measurement, the stimulus protocol, consisting of repetitive depolarization of -10 mV (20 ms in each pulse with a rate of 40 Hz for 1 s), was applied to the tested cells which were voltage-clamped at -80 mV. In accordance with earlier reports [22–25,36], as demonstrated in Figures 4 and 5, during the control period (i.e., neither Tef nor DLT was present), the exponential time course of $I_{Na(T)}$ inactivation

observed in GH₃ cells was observed during a 1-s repetitive depolarization from -80 to -10 mV, and an evolving decaying time constant of 22.1 ± 2.8 ms ($n = 8$) was then yielded. In other words, there appeared to be a progressive current decay (indicated with the dashed arrows in Figure 4A) with a single-exponential process. It also needs to be noted that with cell exposure to DLT ($10 \mu\text{M}$), the time constant of $I_{\text{Na(T)}}$ decaying activated during the same train of depolarizing pulses was increased to 56.4 ± 3.9 ms ($n = 8$), apart from a progressive increase in $I_{\text{Na(L)}}$ or $I_{\text{Na(Tail)}}$ (i.e., appearance of tail current following 1-s PT stimulation) magnitude. Of additional notice, a significant increase in tail I_{Na} ($I_{\text{Na(Tail)}}$) (blue open triangles in Figure 5) with a rising time constant of 87.4 ± 4.6 ms ($n = 8$) was found in the presence of $10 \mu\text{M}$ DLT (Figure 4B,C and Figure 5); however, cell exposure to $10 \mu\text{M}$ Tef resulted in a gradual decay in $I_{\text{Na(L)}}$ with a decaying time constant of 26.3 ± 2.7 ms ($n = 8$). Alternatively, with continued exposure to 10 mM DLT, further addition of Dapa (10 mM) or Ami (10 mM) significantly decreased the time constant of $I_{\text{Na(L)}}$ during PT stimulation. Table 1 summarizes the results showing effects of DLT, DLT plus dapagliflozin (Dapa), DLT plus amiloride (Ami) on either the decaying time constant of $I_{\text{Na(T)}}$ during PT stimulation or the rising time constant of $I_{\text{Na(L)}}$ during the same PT stimulation, as well as the time constant of $I_{\text{Na(Tail)}}$ recovery evoked following PT stimulation.

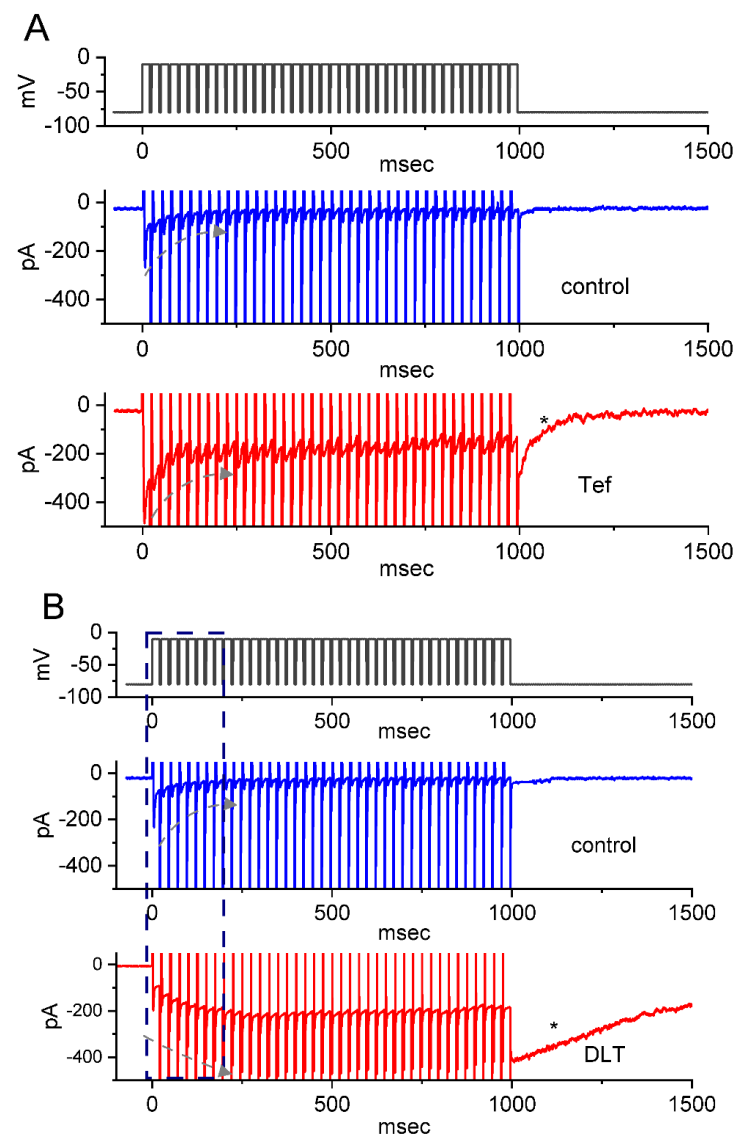


Figure 4. Cont.

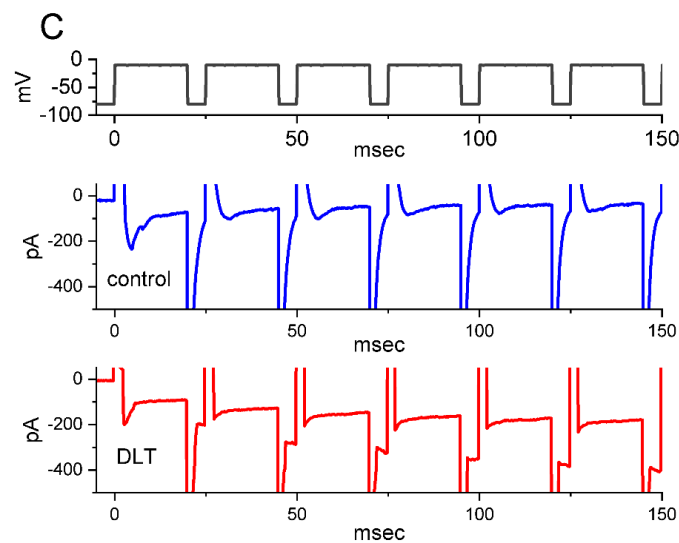


Figure 4. Effects of Tef (A) or DLT (B,C) on I_{Na} evoked by a train of depolarizing pulses (i.e., pulse train [PT] stimulation) in GH₃ cells. The train given consists of 40–20 ms pulses (stepped to -10 mV) separated 5 ms intervals at -80 mV for a total duration of 1 sec. In (A) or (B), exemplar current traces acquired in the control period (i.e., neither Tef nor DLT was present, upper part, blue color) and during cell exposure to $10 \mu\text{M}$ Tef (lower part, red color) or $10 \mu\text{M}$ DLT (lower part, red color) are illustrated, respectively. The voltage-clamp protocol (black color) atop current traces in (A–C) is illustrated. The black dashed arrows in (A) or (B), respectively, indicate the direction of current changes (i.e., either decay or rise) over time in an exponential fashion, while the asterisk shows a large inward deflection following PT stimulation with cell exposure to $10 \mu\text{M}$ Tef (upper) or $10 \mu\text{M}$ DLT (lower). (C) Expanded records (i.e., potential or current traces) from the broken box in (B).

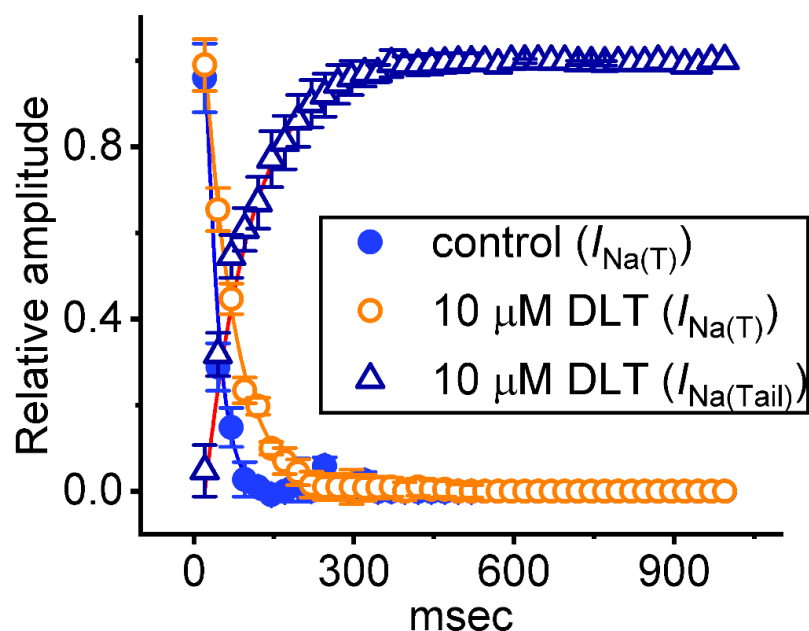


Figure 5. Relationship of $I_{Na(T)}$ or $I_{Na(Tail)}$ versus the pulse train (PT) duration in the absence (blue filled circles) and presence (orange open circles or blue open triangles) of $10 \mu\text{M}$ DLT (mean \pm SEM, $n = 8$ for each point). The observed $I_{Na(T)}$ or $I_{Na(L)}$ was measured as indicated in the right side of Figure 1. The continuous smooth lines, over which the experimental data points are overlaid, were optimally fitted by a single exponential (i.e., exponential decrease or increase). Notably, during PT stimulation, cell exposure to DLT can increase the decaying time constant of $I_{Na(T)}$ inactivation; however, it led to a progressive increase (i.e., staircase increase) in the amplitude of $I_{Na(Tail)}$.

Table 1. Effects of DLT, DLT plus dapagliflozin (Dapa, 10 mM), and DLT plus amiloride (Ami, 10 mM) on either the decaying time constant of $I_{Na(T)}$ during pulse train (PT) stimulation (i.e., cumulative inhibition of $I_{Na(T)}$ during rapid depolarizing stimuli) or the rising time constant of $I_{Na(L)}$ during the same PT stimulation, as well as the time constant of $I_{Na(Tail)}$ recovery evoked following PT stimulation. All values are mean \pm SEM.

	Control	DLT (10 mM)	DLT (10 mM) Plus Dapa (10 mM)	DLT (10 mM) Plus Ami (10 mM)	Cell Number (<i>n</i>)
Decaying time constant of $I_{Na(T)}$	22.1 \pm 2.8 ms	56.4 \pm 3.9 * ms	29.6 \pm 6.1 * ms	30.9 \pm 6.5 * ms	8
Rising time constant of $I_{Na(L)}$	(-)	87.4 \pm 4.6 ms	19.1 \pm 6.1 ** ms	21.1 \pm 6.5 ** ms	8
Recovery time constant of $I_{Na(Tail)}$	25 \pm 3 ms	1.23 \pm 0.19 ⁺ s	0.56 \pm 0.04 ** s	0.58 \pm 0.05 ** s	8

* Significantly different from controls ($p < 0.05$), ** significantly different from DLT (10 mM) alone groups ($p < 0.05$), and ⁺ significantly different from controls ($p < 0.01$). (-) shown in Table 1 indicates that the time constant of $I_{Na(L)}$ during PT stimulation decayed in an exponential manner.

Moreover, with the DLT presence, an exponential increase in $I_{Na(L)}$ during PT stimuli occurring over time was also observed (Figure 4B,C). Following 1-s PT stimulation, as cells were continually exposed to 10 μ M DLT, there appeared to be a large inward current (i.e., $I_{Na(Tail)}$) accompanied by a gradual recovery (indicated with asterisk in Figure 4B) in the second timescale with a recovery time constant of 1.23 \pm 0.19 s ($n = 8$) (Figure 4B,C). The appearance of $I_{Na(Tail)}$ could reflect changes in the magnitude of $I_{Na(P)}$, and the $I_{Na(L)}$ and $I_{Na(P)}$ evoked during an extended period of time were thought to share the same Na_V channels [22,26]. Likewise, with the presence of 10 μ M Tef, the recovery time constant of $I_{Na(Tail)}$ (or $I_{Na(P)}$) acquired following PT stimuli was estimated to be 123 \pm 25 ms ($n = 8$), a value which is different from DLT-induced change in the recovery time constant of $I_{Na(Tail)}$ following PT stimuli. In contrast, during the control period (i.e., neither Tef nor DLT was present), the recovery time constant of the current following PT stimulation was rather small (i.e., 25 \pm 3 ms [$n = 8$]) (Figure 6B). Moreover, with continued presence of DL (10 mM), further addition of either Dapa (10 mM) or Ami (10 mM) significantly attenuated the recovery time constant of $I_{Na(T)}$ evoked following PT stimulation, as summarized in Table 1.

Additionally, with continued exposure to Tef (10 μ M) or DLT (10 μ M), further addition of dapagliflozin (Dap) at a concentration of 10 μ M resulted in an attenuation of the drastic appearance of large inward $I_{Na(Tail)}$ following PT stimuli, as demonstrated by a respective reduction in the recovery time constant of the current to 54 \pm 17 ms ($n = 8$, $p < 0.05$) or 564 \pm 62 ms ($n = 8$, $p < 0.05$) estimated during further presence of Dapa (10 μ M) (Figure 6B). Taken together, these results prompted us to reflect that the presence of DLT can act as a striking slowing the deactivating kinetics of $I_{Na(Tail)}$ (or $I_{Na(P)}$) following return to the holding potential at -80 mV. Therefore, during 1-s PT stimulation, insufficient period of time was allowed for I_{Na} recovery. As a result, particularly during exposure to DLT, single I_{Na} deactivation during PT stimulation presently given (i.e., at a rate of 40 Hz) could be apparently incomplete, thereby leading to frequency-dependent 'accumulation' of the Na_V -channel activated state. Therefore, the response of Tef- and DLT-mediated $I_{Na(L)}$ or $I_{Na(Tail)}$ was overly distinguishable. In other words, one (i.e., the Tef presence) is progressive decay of $I_{Na(L)}$ during a train of depolarizing pulses, while the other (i.e., the DLT presence) exhibits a staircase increase in $I_{Na(L)}$. Moreover, upon continued exposure to 10 μ M DLT, the subsequent addition of Dapa (10 μ M) could measurably attenuate DLT-mediated increase $I_{Na(Tail)}$ during PT stimuli as well as shortened the recovery time constant of $I_{Na(P)}$ following repetitive depolarizing stimuli (Figure 6A,B).

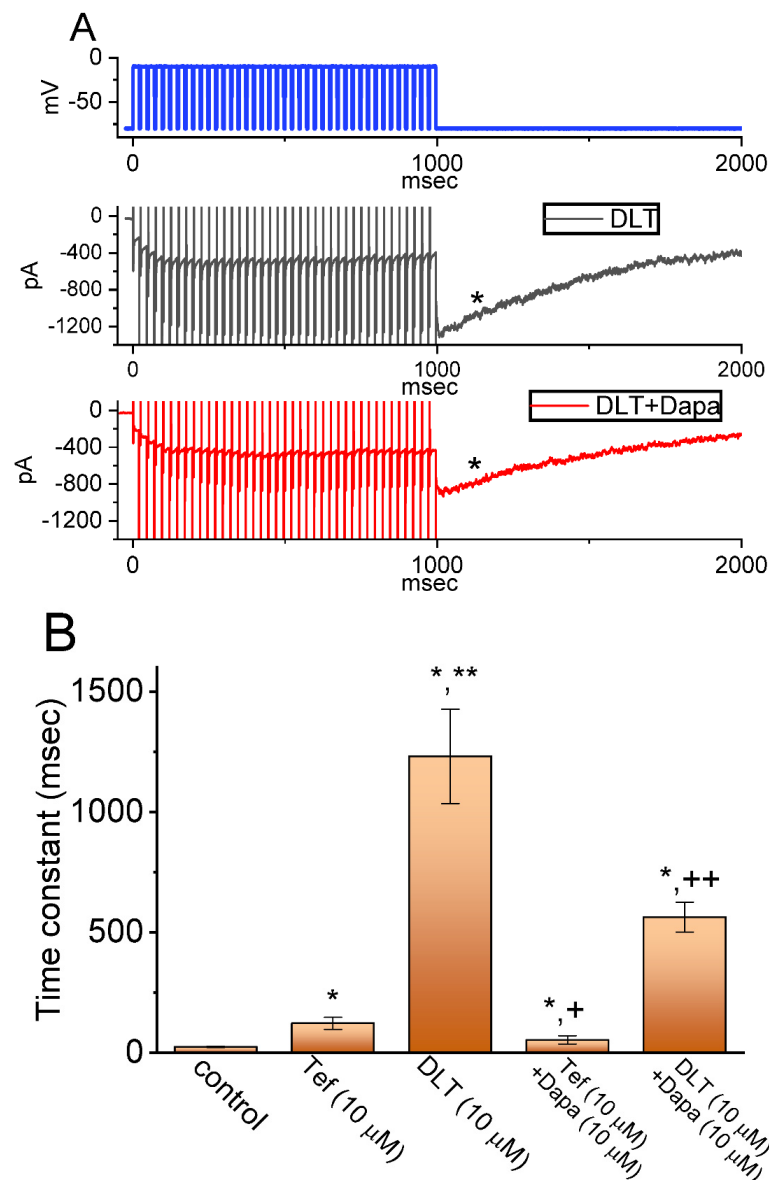


Figure 6. Effect of DLT or DLT plus Dapa on I_{Na} evoked by PT stimulation identified from GH₃ cells. The PT stimulation was applied in exactly the same way as utilized in Figure 4. (A) Exemplar current traces obtained in the presence of DLT (10 μM) alone (black color) or DLT (10 μM) plus Dapa (10 μM) (red color). The upper part shows the voltage-clamp protocol (blue color) given, whereas asterisk denotes the emergence of the current recovery immediately following PT stimulation. (B) Summary bar graph demonstrating effects of Tef, DLT, Tef plus Dapa, and DLT plus Dapa on the recovery time constant of I_{Na} following PT stimulation (mean ± SEM; $n = 8$ for each bar). * Significantly different from control ($p < 0.01$), ** significantly different from Tef (10 μM) alone group ($p < 0.05$), + significantly different from Tef (10 μM) alone group ($p < 0.05$), and ++ significantly different from DLT (10 μM) alone group ($p < 0.05$).

2.5. Effect of Tef or DLT on the Strength of Voltage-Dependent Hysteresis ($Hys_{(V)}$) of Persistent I_{Na} ($I_{Na(P)}$) Elicited by an Upright Isosceles-Triangular Ramp Voltage (V_{ramp})

The nonlinear $Hys_{(V)}$ behavior residing in $I_{Na(P)}$ has been recently disclosed with a figure-of-eight (i.e., ∞-shaped) configuration as current traces were robustly activated by an upright double V_{ramp} (i.e., ascending and descending limbs of triangular V_{ramp}) [33]. In this regard, efforts were made to explore if the existence of Tef or DLT could have any different adjustments on the $Hys_{(V)}$'s behavior elicited in response to such upright V_{ramp} . This separate set of measurements was performed in GH₃ cells which were placed in Ca²⁺-free

Tyrode's solution, and we filled up the measuring electrodes with a solution containing Cs^+ . The tested cells were maintained at -80 mV and an upright double V_{ramp} ranging between -80 and $+50$ mV for a duration of 1 s (i.e., ramp speed of ± 0.26 mV/ms) was afterwards applied to them. As shown in Figure 7A, during cell exposure to Tef ($10 \mu\text{M}$) or DLT ($10 \mu\text{M}$), current traces in response to such triangular V_{ramp} are distinguishable, although two types of hysteretic loops (i.e., low- and high-threshold loops) became overly noticeable during the presence of Tef or DLT. In particular, the strength of low-threshold hysteretic loop during such V_{ramp} became considerably larger in the presence of Tef ($10 \mu\text{M}$), as compared with that during exposure to DLT. For example, as cells were continually exposed to Tef ($10 \mu\text{M}$), the amplitude of $I_{\text{Na(P)}}$ at the descending limb of V_{ramp} (i.e., at the level of -70 mV) resulted in a striking increase by 6.6 folds from 61 ± 9 to 403 ± 24 pA ($n = 8$, $p < 0.05$); conversely, upon the presence of DLT ($10 \mu\text{M}$), $I_{\text{Na(P)}}$ amplitude at the same level was increased only by 1.5 folds (Figure 7C). However, upon cell exposure to Tef ($10 \mu\text{M}$) or DLT ($10 \mu\text{M}$), the $I_{\text{Na(P)}}$ amplitude at the ascending limb (i.e., at -10 mV) was increased to 3.6 or 3.7 folds, respectively, which did not differ significantly between these two compounds. From these data, it was plausible to assume that the strength of $I_{\text{Na(P)}}$'s $\text{Hys}_{\text{(V)}}$ in response to long-lasting double V_{ramp} was susceptible to being enhanced during Tef or DLT presence; moreover, the low-threshold loop of $\text{Hys}_{\text{(V)}}$ appeared to be more sensitive to augmentation by Tef than that by DLT.

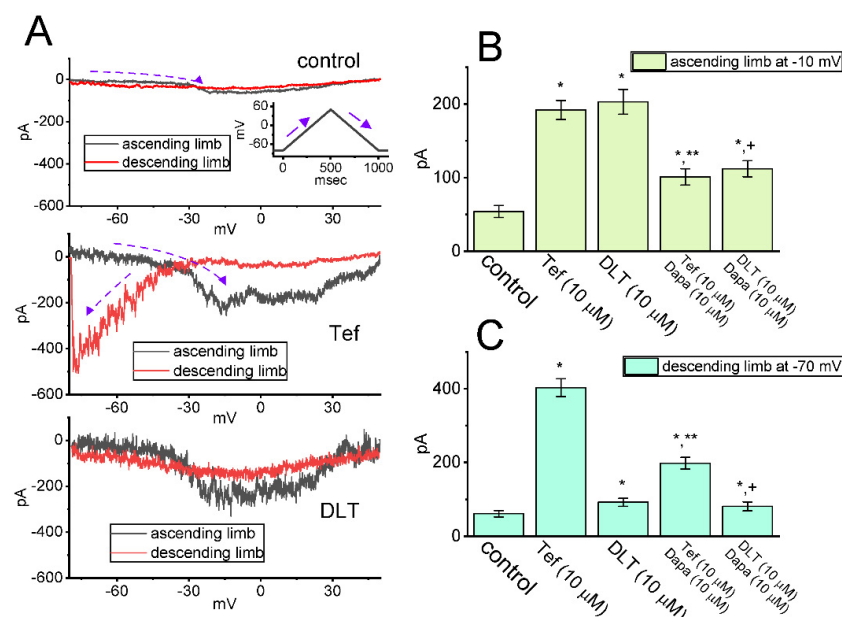


Figure 7. Modifications by Tef or DLT on the strength of voltage-dependent hysteresis ($\text{Hys}_{\text{(V)}}$) in persistent I_{Na} ($I_{\text{Na(P)}}$) present in GH_3 cells. In this set of whole-cell current recordings, the examined cell was voltage-clamped at -80 mV and we then delivered the isosceles-triangular ramp voltage (V_{ramp}) for a duration of 1 s (i.e., a ramp speed of ± 0.26 mV/ms) to activate $I_{\text{Na(P)}}$. (A) Exemplar current traces obtained in the control period (upper) and in the presence of $10 \mu\text{M}$ Tef (middle) or $10 \mu\text{M}$ DLT (lower). The ascending (upsloping) limb is indicated in black color, where the descending (downsloping) one is in the red color. Inset in the upper part of (A) shows the voltage-clamp protocol applied, whereas the dashed arrow indicates the direction of potential or current trajectory by which time goes. In (B) or (C), summary bar graph, respectively, demonstrates the effect of Tef ($10 \mu\text{M}$), DLT ($10 \mu\text{M}$), Tef ($10 \mu\text{M}$) plus Dapa ($10 \mu\text{M}$), and DLT ($10 \mu\text{M}$) plus Dapa ($10 \mu\text{M}$) on $I_{\text{Na(P)}}$ amplitude activated by upsloping (at -10 mV) or downsloping limb (at the level of -70 mV) of double V_{ramp} (mean \pm SEM; $n = 8$ for each bar). * Significantly different from control ($p < 0.05$), ** significantly different from Tef ($10 \mu\text{M}$) alone group ($p < 0.05$), and + significantly different from DLT ($10 \mu\text{M}$) alone group ($p < 0.05$).

3. Discussion

In the current investigations together with previous studies, we provided the evidence to unveil that the presence of DLT, known to be a type II pyrethroid, was able to exert stimulatory actions on vastly different types of I_{Na} , including $I_{Na(T)}$, $I_{Na(L)}$, $I_{Na(Tail)}$, and $I_{Na(P)}$, seen in pituitary tumor (GH₃) cells. It is likely, therefore, that the endocrine disrupting potential caused by the existence of DLT or other structurally similar pyrethroids, as demonstrated recently [2,16,20,27,37–41], could be highly linked to the excitatory actions on varying types of I_{Na} presented herein, presuming that similar pharmacological or toxicological actions take place in variable types of endocrine or neuroendocrine cells present in vivo [2,3,7,11,13,42], although pyrethroids are thought to be around 2250 times more toxic than mammals [12,13].

Upon cell exposure to DLT, the observed $I_{Na(L)}$ activated in response to short depolarizing step was noticed to be stimulated to a greater extent than the $I_{Na(T)}$. The EC₅₀ values required for DLT-stimulated $I_{Na(T)}$ and $I_{Na(L)}$ in GH₃ cells were estimated to be 11.2 and 2.5 μ M, these values which was noted to differ significantly by 4.5 folds (Figure 1). However, the further addition of chlorotoxin (ChloroTx), still in continued presence of tefluthrin (Tef) or DLT, failed to modify Tef- or DLT-stimulated $I_{Na(L)}$, although either dapagliflozin (Dapa) or amiloride could effectively reverse their increase in $I_{Na(L)}$ amplitude. Tef is a Type I pyrethroid insecticide [8,10,26]. The overall steady-state I - V relationship of $I_{Na(T)}$ or $I_{Na(L)}$ during exposure to DLT remained unchanged; furthermore, the inactivation time course of $I_{Na(T)}$ during brief step depolarizing did not differ between the absence and presence of DLT. However, the magnitude of $I_{Na(T)}$ following the PT stimulation (i.e., 40-Hz repetitive depolarizing pulse) tended to be pronouncedly larger as well as its decaying time course became slowed in the presence of Tef or DLT (Figure 4).

It needs to be mentioned that a large appearance of inward current (i.e., $I_{Na(P)}$) following such PT stimulation clearly emerged during the presence of Tef or DLT, while a rather small transient current following the same PT stimuli was observed during the control conditions (i.e., neither Tef nor DLT was present). The larger magnitude of inward current immediately following PT stimuli by adding DLT was noted as compared to that by Tef. Furthermore, the exposure to Tef markedly rendered the inactivation time course of $I_{Na(T)}$ during rapid membrane depolarization to become slowed, whereas DLT itself had minimal interference with the inactivation time constant of the current. However, the DLT existence, a progressive elevation of $I_{Na(L)}$ and $I_{Na(Tail)}$ during a train of repetitive depolarizations; moreover, it induced a larger tail I_{Na} following repetitive depolarizations. The experimental results can be interpreted to mean that, upon continued exposure to DLT, the I_{Na} deactivation elicited during PT stimuli could be apparently incomplete, thus leading to rate-dependent ‘accumulation’ of the Na_v channel activated state. The slowed inactivation caused by the exposure to Tef thus reflects that the barrier for going from the open to the inactivated state of the Na_v channel tends to be higher during its presence. The α -cyano-3-phenoxybenzyl group present in the DLT molecule tends to be a notable structure required preferentially for open/resting state of the channel.

Earlier reports have demonstrated the effectiveness of DLT either in inducing the raise in Ca²⁺ transient or exert anti-neoplastic actions in different types of neoplastic cells, including liver, oral, and prostate cancer cells, and Jurkat-J6 cell cells [43–48]. The functional expression of Na_v channels has also been reported in different neoplastic cells, including prostate cancer and glioma cells [45,49–52]. As such, whether DLT-mediated modifications on I_{Na} presented herein can be responsible for the actions of DLT or other structurally similar pyrethroids on intracellular Ca²⁺ or aberrant growth in neoplastic cells [44] is worth pursuing further.

Earlier reports have demonstrated the effectiveness of pyrethroids (e.g., DLT, esfenvalerate, or permethrin) in increasing long-term potentiation recorded in CA1 hippocampal region [53–56]. Indeed, a brief period of high-frequency electrical activity applied artificially to a neuronal pathway is expected to enhance the strength of synapses for various periods of time, which is called long-term potentiation. However, it needs to be stressed that with

cell exposure to either Tef or DLT, following 1-s PT stimulation from -80 to -10 mV, a large inward current (i.e., $I_{\text{Na(P)}}$) with slowly decaying process was considerably observed (Figure 4A,B). Under such scenario, the observed induction of long-term potentiation (i.e., facilitation of synaptic transmitter [e.g., glutamate] release) evoked during high-frequency stimulation could have been seriously disturbed or even overestimated by the present findings showing a large recovery time course of I_{Na} emerging following PT stimulation in situations where cells present in tissue preparations were exposed to either Tef or DLT.

Previous studies have demonstrated that pyrethroids could affect transepithelial ion transport in the external layers of the skin and the further addition of amiloride could regulate pyrethroids-mediated change in such transepithelial ion transport [16,57]. In this study, the subsequent addition of amiloride can attenuate DLT-induced increase in $I_{\text{Na(L)}}$ measured from GH₃ cells; however, further application of chlorotoxin (ChloroTx) had no effect on DLT- or Tef-stimulated I_{Na} . Moreover, further addition of ChloroTx failed to modify changes in DLT- or Tef-stimulated I_{Na} during PT stimulation; however, subsequent application of either Dapa or amiloride could significantly attenuate DLT and Tef-stimulated I_{Na} by the same stimulation protocol. Therefore, the amiloride-mediated effect on the modifications by pyrethroids of ion transport through rabbit skin is likely associated with its direct inhibitory action on $I_{\text{Na(L)}}$.

The ability of pyrethroids (e.g., DLT) to augment Cl^- currents has been previously demonstrated [14,16]. In our study, the subsequent addition of ChloroTx, an inhibitor of Cl^- currents, failed to modify DLT-stimulated $I_{\text{Na(T)}}$ or $I_{\text{Na(L)}}$ in GH₃ cells (Figure 2). However, the further application of dapagliflozin (Dapa) or amiloride can effectively attenuate DLT-activated $I_{\text{Na(L)}}$ or $I_{\text{Na(P)}}$. Dapa was recently demonstrated to ameliorate Tef-augmented Hys_(V) strength of $I_{\text{Na(P)}}$ activated by double V_{ramp} [33]. Therefore, DLT-mediated stimulation of $I_{\text{Na(T)}}$, $I_{\text{Na(L)}}$, and $I_{\text{Na(P)}}$ demonstrated herein is unlikely to be attributed to its activation of Cl^- current.

Work in our laboratory has demonstrated the non-equilibrium Hys_(V) behavior of $I_{\text{Na(P)}}$ activated by the upright isosceles-triangular V_{ramp} [33]. The results indicated that there was a striking voltage dependence of such V_{ramp} -evoked $I_{\text{Na(P)}}$ [29,33]. The experimental data also showed two types of Hys_(V) loops (i.e., a high-threshold counterclockwise followed by a low-threshold clockwise loop) with a figure-of-eight (i.e., ∞) configuration, which is reminiscent of the dynamics of the Lorenz-like motion [58]. Alternatively, with GH₃-cell exposure to Tef or DLT, the Hys_(V) motion of $I_{\text{Na(P)}}$ activated by the upsloping (ascending) and downsloping (descending) ends of such double V_{ramp} as a function of time was noticed to move in both counterclockwise and clockwise directions (Figure 7A). In particular, one activated during the ascending limb of double V_{ramp} is called a high-threshold counterclockwise loop with a peak of around -10 mV, while the other evoked by the descending limb of V_{ramp} is a low-threshold clockwise loop with a peak falling at around -70 mV [33]. Moreover, as compared with the effect of DLT on Hys_(V)'s strength of $I_{\text{Na(P)}}$, the exposure to Tef could augment Hys_(V)'s strength at low-threshold loop to a greater extent than that observed at high-threshold loop. However, with continued presence of either Tef or DLT, the further addition of Dapa could attenuate their stimulation of Hys_(V) strength in GH₃ cells. Thus, the presence of Tef could slow the inactivation time course of $I_{\text{Na(T)}}$ activated by rapid step depolarization as well as augment magnitude of $I_{\text{Na(P)}}$'s low-threshold loop of Hys_(V) responding to double V_{ramp} . Conversely, as cells were exposed to DLT, the $I_{\text{Na(T)}}$ inactivation time course during step depolarization was found to remain unchanged, and the increased strength of low-threshold Hys_(V) loop during double V_{ramp} was relatively smaller in its presence. It is therefore plausible to assume that the low-threshold loop of $I_{\text{Na(P)}}$'s Hys_(V) activated during the downsloping end of double V_{ramp} could be closely linked to the extent of the inactivation time course of $I_{\text{Na(T)}}$.

4. Conclusions

The modifications by DLT and Tef on the magnitude, gating kinetics, frequency dependence, and Hys_(V) strength of I_{Na} in electrically excitable cells are noticeably different.

The variable actions of pyrethroids presented here would be of clinical, pharmacological, and toxicological relevance [3].

5. Materials and Methods

5.1. Chemicals, Drugs, Reagents, and Solution Used in This Work

Deltamethrin (DLT, decamethrin, $C_{22}H_{19}Br_2NO_3$, IUPAC name: [(S)-cyano-(3-phenoxyphenyl)methyl](1R,3R)-3-(2,2-dibromoethenyl)-2,2-dimethylcyclopropane-1-carboxylate, (S)- α -cyano-3-phenoxybenzyl-cis-(1R,3R)-3(2,2-dibromovinyl)(2,2-dimethyl-cyclopropane-carboxylate) was acquired from MedChemExpress (Asia Biomed Inc., Taipei, Taiwan), dapagliflozin (Dapa, Foxiga[®]) was from Cayman (Ann Arbo, MI), while amiloride, tetraethylammonium chloride (TEA), tetrodotoxin (TTX), and tefluthrin (Tef) were from Sigma-Aldrich (Genechain, Kaohsiung, Taiwan). Chlorotoxin was a kind gift from Professor Dr. Woei-Jer Chuang (Department of Biochemistry, National Cheng Kung University Medical College, Tainan, Taiwan). Because of a highly nonpolar nature of low water solubility (Laskowski, 2002), the stock solution of DLT (10 mM) was prepared by dissolving it in dimethylsulfoxide (DMSO), and it was wrapped in aluminum foil and then kept under $-20\text{ }^{\circ}\text{C}$ for long-term storage. Unless specified otherwise, growth media (e.g., Ham's F-12 medium), fetal or horse bovine serum, trypsin/EDTA, and L-glutamine were mostly acquired from HyClone[™] (Thermo Fisher, Kaohsiung, Taiwan), while other chemicals or reagents were from Sigma-Aldrich or Merck (Genechain), and they were of laboratory grade and taken from standard sources.

The standard extracellular solution (i.e., normal Tyrode's solution) used in this study had the ionic compositions containing (in mM): NaCl 136.5, $CaCl_2$ 1.8, KCl 5.4, $MgCl_2$ 0.53, glucose 5.5, HEPES 5.5, and the solution pH was titrated to 7.4 by adding NaOH. The composition of Ca^{2+} -free Tyrode's solution used for the measurement of I_{Na} (e.g., $I_{Na(T)}$, $I_{Na(L)}$, $I_{Na(P)}$, and $I_{Na(Tail)}$) was the same as normal Tyrode's solution in which $CaCl_2$ was removed. For the experiments on recording I_{Na} , the electrode used was filled up with the internal pipette solution containing (in mM): Cs-aspartate 130, CsCl 20, KH_2PO_4 1. $MgCl_2$, Na_2ATP 3, Na_2GTP 0.1, and HEPES 5, and the pH was then adjusted to 7.2 with CsOH. The twice-distilled water used for the experiments was deionized with a Milli-Q ion exchange and activated carbon cartridge treatment system (Merck, Tainan, Taiwan).

5.2. Cell Preparation

Clonal pituitary (GH₃) somatolactotrophs, originally acquired from the Bioresources Collection and Research Center ([BCRC-60015], <http://catalog.bcrc.firdi.org.tw/BrcrContent?bid=60015>) (access on 19 September 2022), Hsinchu, Taiwan), were revived and cultured in Ham's F-12 growth medium, which was supplemented with 15% heat-inactivated horse serum (*v/v*), 2.5 % fetal calf serum (*v/v*), and 2 mM L-glutamine. They were commonly incubated at $37\text{ }^{\circ}\text{C}$ in monolayer cultures in 50-mL plastic culture flasks in a humidified environment of 5% CO_2 /95% air. It was confirmed that this cell line can continually secrete prolactin. We carried out electrical recordings 5 or 6 days after cells underwent subculture (60–70% confluence).

5.3. Electrophysiological Measurements (Patch-Clamp Current Recordings)

In the few hours before the experiments, GH₃ cells were detached from culture dishes with a 1% trypsin/EDTA solution, and a few drops of cell suspension ($\sim 10^6$ /mL) was rapidly placed in a custom-built chamber mounted on the stage of a DM-IL inverted phase-contrast microscope (Leica; Major Instruments, Kaohsiung, Taiwan). We bathed cells at room temperature ($20\text{--}25\text{ }^{\circ}\text{C}$) in the extracellular solution (i.e., normal Tyrode's solution), the ionic compositions of which are described above. Before each experiment, cells were allowed to settle on the chamber's bottom. The recording pipettes were pulled from Kimax[®]-51 borosilicate glass tube (#DWK34500-99; Kimble[®], Merck, Tainan, Taiwan) and they were then polished to reach the resistances ranging between 3 and $5\text{ M}\Omega$. During each measurement, the electrode was mounted in an air-tight holder, which had a suction port on

the side, and a silver-chloride wire was used to make good contact with the internal pipette solution. We recorded varying types of ionic currents (e.g., I_{Na}) with the whole-cell mode of a modified patch-clamp technique by using an RK-400 patch amplifier (Bio-Logic, Claix, France), as dealt with in our previous works [26,36,59]. All recordings were conducted inside a noise-proof Faraday cage. The junction potentials that commonly develop when the compositions of the pipette internal solution are different from those in the bath were zeroed shortly before giga- Ω formation was made, and the whole-cell data were corrected. As pulse train (PT) stimulation was applied to the tested cell, we used an Astro-Med Grass S88X dual output pulse stimulator (Grass; KYS Technology, Tainan, Taiwan).

5.4. Data Recordings and Processing

Throughout the recording period, the signal output (i.e., potential and current traces) was monitored and digitized online at 10 kHz or more in an ASUS ExpertBook laptop computer (Yuan-Dai, Tainan, Taiwan). For analog-to-digital (A/D) and digital-to-analog (D/A) conversion, a Digidata[®] 1550B converter equipped with the computer was controlled by pCLAMP[™] 10.6 program run under Microsoft Windows 7 (Redmond, WA, USA). Current signals were low-pass filtered at 2 kHz by using a FL-4 four-pole Bessel filter (Dagan, Minneapolis, MN, USA). The voltage-clamp protocols with manifold rectangular or ramp waveforms were designed, and they were then given to the examined cell through D/A conversion.

5.5. Data Analyses for Whole-Cell Ionic Currents

To establish concentration-dependent stimulation of DLT on the amplitude of $I_{\text{Na(T)}}$ or $I_{\text{Na(L)}}$, we bathed GH₃ cells in Ca²⁺-free Tyrode's solution which contained 10 mM tetraethylammonium chloride (TEA). During the recording period, we voltage-clamped each cell at -80 mV, and a brief step depolarization to -10 mV for a 20 ms at a rate 0.2 Hz was applied to evoke I_{Na} . The $I_{\text{Na(T)}}$ magnitude was measured as the peak amplitude of I_{Na} at the beginning of depolarizing pulse was subtracted from the sustained I_{Na} (i.e., $I_{\text{Na(L)}}$), while the $I_{\text{Na(L)}}$ magnitude was measured at the end of 20-ms depolarizing pulse in situations where different DLT concentrations were cumulatively given (as indicated in the right side of Figure 1A). The total amplitude of I_{Na} ($I_{\text{Na(Tot)}}$) taken from each step depolarization is equal to $I_{\text{Na(T)}}$ plus $I_{\text{Na(L)}}$. The amplitude of $I_{\text{Na(L)}}$ obtained during the presence of DLT at a concentration of 100 μM was considered as 100% and we then compared current magnitudes (i.e., $I_{\text{Na(T)}}$ and $I_{\text{Na(L)}}$) during cell exposure to varying concentrations of DLT. The concentration-dependent stimulation by DLT of $I_{\text{Na(T)}}$ or $I_{\text{Na(L)}}$ observed in GH₃ cells was determined by fitting experimental data set to a modified Hill function [10,25], which can be given as follows.

$$\text{percentage increase (\%)} = \langle E_{\text{max}} \times [\text{DLT}]^{n_{\text{H}}} \rangle / \langle \text{EC}_{50}^{n_{\text{H}}} + [\text{DLT}]^{n_{\text{H}}} \rangle$$

In this equation, [DLT] = the deltamethrin (DLT) concentration given; n_{H} = the Hill coefficient (i.e., coefficient for cooperativity); EC_{50} = the concentration required for a 50% stimulation of $I_{\text{Na(T)}}$ or $I_{\text{Na(L)}}$ amplitude activated in response to short depolarizing step from -80 to -10 mV; and E_{max} = maximal stimulation of $I_{\text{Na(T)}}$ or $I_{\text{Na(L)}}$ produced by the DLT presence.

5.6. Curve-Fitting Approximations and Statistical Analyses Used in This Work

To determine the model parameters, linear or nonlinear curve-fitting to the experimental data set presently obtained was optimally fitted with least-squares minimization procedure by using manifold analytical tools, such as the Microsoft "Solver" built in Excel[®] 2022 (Microsoft) and OriginPro[®] 2022 program (OriginLab[®]; Scientific Formosa, Kaoshiung, Taiwan). The experimental results are presented as the mean \pm standard error of the mean (SEM). The size of independent observations (n) is indicated in cell numbers collected during the measurements. The data distribution obtained presently was found to satisfy the tests for normality. Paired or unpaired t -tests were used for comparison

between the two different groups; however, for comparison among more than two groups, we carried out analysis of variance (for one- or two-way ANOVA) with or without repeated measure followed by a post hoc Fisher's least-significance difference test for multiple-range comparisons. A statistical significance (indicated with *, **, +, or ++ in the figures) was considered when $p < 0.01$ or < 0.05 .

Author Contributions: Conceptualization, S.-N.W., M.-H.L., J.-F.L., C.-L.W., H.-Y.C. and M.-C.Y.; Methodology, S.-N.W.; Software, S.-N.W.; Validation, M.-H.L., J.-F.L., C.-L.W., M.-C.Y., H.-Y.C. and S.-N.W.; Formal analysis, S.-N.W.; Investigation, M.-C.Y. and S.-N.W.; Resources, S.-N.W.; Data curation, S.-N.W.; Writing—original draft preparation, S.-N.W.; Writing—review and editing, M.-H.L., J.-F.L., C.-L.W., H.-Y.C., M.-C.Y. and S.-N.W.; Visualization, M.-C.Y., H.-Y.C. and S.-N.W.; Supervision, M.-H.L., J.-F.L., C.-L.W. and S.-N.W.; Project administration, M.-H.L., J.-F.L., C.-L.W. and S.-N.W.; Funding acquisition, M.-H.L., J.-F.L. and S.-N.W. All authors have read and agreed to the published version of the manuscript.

Funding: The research detailed in the present work was supported partly by grants from the National Science and Technology Council, Taiwan (MOST-110-2320-B-006-028 and MOST-111-2320-B-006-028) and Ditmanson Medical Foundation Chia-Yi Christian Hospital Research Program. The funders in this work are not involved in the study design, data collection, analyses, or interpretation.

Institutional Review Board Statement: Not applicable.

Informed Consent Statement: Not applicable.

Data Availability Statement: The original data is available upon reasonable request to the corresponding author.

Acknowledgments: The authors thank Hsin-Yen Cho for her contribution to the earlier experiments.

Conflicts of Interest: All the authors report no declaration that is directly relevant to this work.

Abbreviations

DLT	deltamethrin
ChloroTx	chlorotoxin
Dapa	dapagliflozin
EC ₅₀	concentration required for half-maximal stimulation
Hys _(V)	voltage-dependent hysteresis
<i>I</i> - <i>V</i> relationship	current versus voltage relationship
<i>I</i> _{Na}	voltage-gated Na ⁺ current
<i>I</i> _{Na(L)}	late Na ⁺ current
<i>I</i> _{Na(P)}	persistent Na ⁺ current
<i>I</i> _{Na(Tot)}	total Na ⁺ current (i.e., <i>I</i> _{Na(T)} plus <i>I</i> _{Na(L)})
<i>I</i> _{Na(Tail)}	tail Na ⁺ current
Na _V channel	voltage-gated Na ⁺ channel
PT stimulation	pulse train stimulation
Tef	tefluthrin
V _{ramp}	ramp voltage

References

1. Laskowski, D.A. Physical and chemical properties of pyrethroids. *Rev. Environ. Contam. Toxicol.* **2002**, *174*, 49–170. [[PubMed](#)]
2. Bradberry, S.M.; Cage, S.A.; Proudfoot, A.T.; Vale, J.A. Poisoning due to pyrethroids. *Toxicol. Rev.* **2005**, *24*, 93–106. [[CrossRef](#)] [[PubMed](#)]
3. Dhiman, S.; Yadav, K.; Acharya, B.N.; Nagar, D.P.; Rao Ghorpade, R. Deltamethrin Contact Exposure Mediated Toxicity and Histopathological Aberrations in Tissue Systems of Public Health Importance Cockroach Species *Periplaneta americana* and *Blattella germanica*. *Front. Physiol.* **2022**, *13*, 926267. [[CrossRef](#)]
4. Eads, D.; Livieri, T.; Tretten, T.; Hughes, J.; Kaczor, N.; Halsell, E.; Grassel, S.; Dobesh, P.; Childers, E.; Lucas, D.; et al. Assembling a safe and effective toolbox for integrated flea control and plague mitigation: Fipronil experiments with prairie dogs. *PLoS ONE* **2022**, *17*, e0272419. [[CrossRef](#)]
5. Ma, C.; Wei, D.; Liu, P.; Fan, K.; Nie, L.; Song, Y.; Wang, M.; Wang, L.; Xu, Q.; Wang, J.; et al. Pesticide Residues in Commonly Consumed Vegetables in Henan Province of China in 2020. *Front. Public Health* **2022**, *10*, 901485. [[CrossRef](#)]

6. Tabarean, I.V.; Narahashi, T. Potent modulation of tetrodotoxin-sensitive and tetrodotoxin-resistant sodium channels by the type II pyrethroid deltamethrin. *J. Pharmacol. Exp. Ther.* **1998**, *284*, 958–965.
7. Tan, J.; Soderlund, D.M. Divergent actions of the pyrethroid insecticides S-bioallethrin, tefluthrin, and deltamethrin on rat Na(v)1.6 sodium channels. *Toxicol. Appl. Pharmacol.* **2010**, *247*, 229–237. [[CrossRef](#)] [[PubMed](#)]
8. McCavera, S.J.; Soderlund, D.M. Differential state-dependent modification of inactivation-deficient Nav1.6 sodium channels by the pyrethroid insecticides S-bioallethrin, tefluthrin and deltamethrin. *Neurotoxicology* **2012**, *33*, 384–390. [[CrossRef](#)]
9. James, T.F.; Nenov, M.N.; Tapia, C.M.; Lecchi, M.; Koshy, S.; Green, T.A.; Laezza, F. Consequences of acute Na(v)1.1 exposure to deltamethrin. *Neurotoxicology* **2017**, *60*, 150–160. [[CrossRef](#)]
10. So, E.C.; Wu, S.N.; Lo, Y.C.; Su, K. Differential regulation of tefluthrin and telmisartan on the gating charges of I(Na) activation and inactivation as well as on resurgent and persistent I_{Na} in a pituitary cell line (GH₃). *Toxicol. Lett.* **2018**, *285*, 104–112. [[CrossRef](#)]
11. Breckenridge, C.B.; Holden, L.; Sturgess, N.; Weiner, M.; Sheets, L.; Sargent, D.; Soderlund, D.M.; Choi, J.S.; Symington, S.; Clark, J.M.; et al. Evidence for a separate mechanism of toxicity for the Type I and the Type II pyrethroid insecticides. *Neurotoxicology* **2009**, *30* (Suppl. 1), S17–S31. [[CrossRef](#)] [[PubMed](#)]
12. Chrustek, A.; Holyńska-Iwan, I.; Dziembowska, I.; Bogusiewicz, J.; Wróblewski, M.; Cwynar, A.; Olszewska-Słonina, D. Current Research on the Safety of Pyrethroids Used as Insecticides. *Medicina* **2018**, *54*, 61. [[CrossRef](#)]
13. Williams, M.T.; Gutierrez, A.; Vorhees, C.V. Effects of Acute Deltamethrin Exposure in Adult and Developing Sprague Dawley Rats on Acoustic Startle Response in Relation to Deltamethrin Brain and Plasma Concentrations. *Toxicol. Sci.* **2019**, *168*, 61–69. [[CrossRef](#)] [[PubMed](#)]
14. Forshaw, P.J.; Lister, T.; Ray, D.E. Inhibition of a neuronal voltage-dependent chloride channel by the type II pyrethroid, deltamethrin. *Neuropharmacology* **1993**, *32*, 105–111. [[CrossRef](#)]
15. Burr, S.A.; Ray, D.E. Structure-activity and interaction effects of 14 different pyrethroids on voltage-gated chloride ion channels. *Toxicol. Sci.* **2004**, *77*, 341–346. [[CrossRef](#)] [[PubMed](#)]
16. Holyńska-Iwan, I.; Bogusiewicz, J.; Chajdas, D.; Szewczyk-Golec, K.; Lampka, M.; Olszewska-Słonina, D. The immediate influence of deltamethrin on ion transport through rabbit skin. An in vitro study. *Pestic. Biochem. Physiol.* **2018**, *148*, 144–150. [[CrossRef](#)] [[PubMed](#)]
17. Costa, L.G. The neurotoxicity of organochlorine and pyrethroid pesticides. *Handb. Clin. Neurol.* **2015**, *131*, 135–148. [[PubMed](#)]
18. Van Goor, F.; Zivadinovic, D.; Stojilkovic, S.S. Differential expression of ionic channels in rat anterior pituitary cells. *Mol. Endocrinol.* **2001**, *15*, 1222–1236. [[CrossRef](#)]
19. Jukič, M.; Kikelj, D.; Anderluh, M. Isoform selective voltage-gated sodium channel modulators and the therapy of pain. *Curr. Med. Chem.* **2014**, *21*, 164–186. [[CrossRef](#)]
20. Guéroux, N.C.; Monteil, A.; Lory, P. Sodium background currents in endocrine/neuroendocrine cells: Towards unraveling channel identity and contribution in hormone secretion. *Front. Neuroendocrinol.* **2021**, *63*, 100947. [[CrossRef](#)]
21. Catterall, W.A. Forty Years of Sodium Channels: Structure, Function, Pharmacology, and Epilepsy. *Neurochem. Res.* **2017**, *42*, 2495–2504. [[CrossRef](#)] [[PubMed](#)]
22. Taddese, A.; Bean, B.P. Subthreshold sodium current from rapidly inactivating sodium channels drives spontaneous firing of tuberomammillary neurons. *Neuron* **2002**, *33*, 587–600. [[CrossRef](#)] [[PubMed](#)]
23. Huang, C.W.; Hung, T.Y.; Wu, S.N. The inhibitory actions by lacosamide, a functionalized amino acid, on voltage-gated Na⁺ currents. *Neuroscience* **2015**, *287*, 125–136. [[CrossRef](#)] [[PubMed](#)]
24. Navarro, M.A.; Salari, A.; Lin, J.L.; Cowan, L.M.; Penington, N.J.; Milescu, M.; Milescu, L.S. Sodium channels implement a molecular leaky integrator that detects action potentials and regulates neuronal firing. *Elife* **2020**, *9*, e54940. [[CrossRef](#)]
25. Wu, P.M.; Lai, P.C.; Cho, H.Y.; Chuang, T.H.; Wu, S.N.; Tu, Y.F. Effective Perturbations by Phenobarbital on I(Na), I(K(erg)), I(K(M)) and I(K(DR)) during Pulse Train Stimulation in Neuroblastoma Neuro-2a Cells. *Biomedicines* **2022**, *10*, 1968. [[CrossRef](#)]
26. Wu, S.N.; Chen, B.S.; Hsu, T.I.; Peng, H.; Wu, Y.H.; Lo, Y.C. Analytical studies of rapidly inactivating and noninactivating sodium currents in differentiated NG108-15 neuronal cells. *J. Theor. Biol.* **2009**, *259*, 828–836. [[CrossRef](#)]
27. Stojilkovic, S.S.; Bjelobaba, I.; Zemkova, H. Ion Channels of Pituitary Gonadotrophs and Their Roles in Signaling and Secretion. *Front. Endocrinol.* **2017**, *8*, 126. [[CrossRef](#)]
28. Zhang, J.; Chen, X.; Eaton, M.; Wu, J.; Ma, Z.; Lai, S.; Park, A.; Ahmad, T.S.; Que, Z.; Lee, J.H.; et al. Severe deficiency of the voltage-gated sodium channel Na(V)1.2 elevates neuronal excitability in adult mice. *Cell Rep.* **2021**, *36*, 109495. [[CrossRef](#)]
29. Hsu, C.L.; Zhao, X.; Milstein, A.D.; Spruston, N. Persistent Sodium Current Mediates the Steep Voltage Dependence of Spatial Coding in Hippocampal Pyramidal Neurons. *Neuron* **2018**, *99*, 147–162.e8. [[CrossRef](#)]
30. Gutiérrez, Y.; Tomé, H.V.V.; Guedes, R.N.C.; Oliveira, E.E. Deltamethrin toxicity and impaired swimming behavior of two backswimmer species. *Environ. Toxicol. Chem.* **2017**, *36*, 1235–1242. [[CrossRef](#)]
31. Vega, A.V.; Espinosa, J.L.; López-Domínguez, A.M.; López-Santiago, L.F.; Navarrete, A.; Cota, G. L-type calcium channel activation up-regulates the mRNAs for two different sodium channel alpha subunits (Nav1.2 and Nav1.3) in rat pituitary GH3 cells. *Brain Res. Mol. Brain Res.* **2003**, *116*, 115–125. [[CrossRef](#)] [[PubMed](#)]
32. Philippaert, K.; Kalyaanamoorthy, S.; Fatehi, M.; Long, W.; Soni, S.; Byrne, N.J.; Barr, A.; Singh, J.; Wong, J.; Palechuk, T.; et al. Cardiac Late Sodium Channel Current Is a Molecular Target for the Sodium/Glucose Cotransporter 2 Inhibitor Empagliflozin. *Circulation* **2021**, *143*, 2188–2204. [[CrossRef](#)] [[PubMed](#)]

33. Wu, S.N.; Wu, C.L.; Cho, H.Y.; Chiang, C.W. Effective Perturbations by Small-Molecule Modulators on Voltage-Dependent Hysteresis of Transmembrane Ionic Currents. *Int. J. Mol. Sci.* **2022**, *23*, 9453. [[CrossRef](#)] [[PubMed](#)]
34. Tsai, D.; Morley, J.W.; Suaning, G.J.; Lovell, N.H. Frequency-dependent reduction of voltage-gated sodium current modulates retinal ganglion cell response rate to electrical stimulation. *J. Neural Eng.* **2011**, *8*, 066007. [[CrossRef](#)] [[PubMed](#)]
35. Muralidharan, M.; Guo, T.; Shivdasani, M.N.; Tsai, D.; Fried, S.; Li, L.; Dokos, S.; Morley, J.W.; Lovell, N.H. Neural activity of functionally different retinal ganglion cells can be robustly modulated by high-rate electrical pulse trains. *J. Neural Eng.* **2020**, *17*, 045013. [[CrossRef](#)]
36. Shiau, A.L.; Liao, C.S.; Tu, C.W.; Wu, S.N.; Cho, H.Y.; Yu, M.C. Characterization in Effective Stimulation on the Magnitude, Gating, Frequency Dependence, and Hysteresis of I(Na) Exerted by Picaridin (or Icaridin), a Known Insect Repellent. *Int. J. Mol. Sci.* **2022**, *23*, 9696. [[CrossRef](#)]
37. Xue, N.; Li, F.; Hou, H.; Li, B. Occurrence of endocrine-disrupting pesticide residues in wetland sediments from Beijing, China. *Environ. Toxicol. Chem.* **2008**, *27*, 1055–1062. [[CrossRef](#)]
38. Eni, G.; Ibor, O.R.; Andem, A.B.; Oku, E.E.; Chukwuka, A.V.; Adeogun, A.O.; Arukwe, A. Biochemical and endocrine-disrupting effects in *Clarias gariepinus* exposed to the synthetic pyrethroids, cypermethrin and deltamethrin. *Comp. Biochem. Physiol. C Toxicol. Pharmacol.* **2019**, *225*, 108584. [[CrossRef](#)]
39. Holyńska-Iwan, I.; Szewczyk-Golec, K. Pyrethroids: How They Affect Human and Animal Health? *Medicina* **2020**, *56*, 582. [[CrossRef](#)]
40. Knapke, E.T.; Magalhaes, D.P.; Dalvie, M.A.; Mandrioli, D.; Perry, M.J. Environmental and occupational pesticide exposure and human sperm parameters: A Navigation Guide review. *Toxicology* **2022**, *465*, 153017. [[CrossRef](#)]
41. Yang, Y.; Wang, C.; Shen, H.; Fan, H.; Liu, J.; Wu, N. Cis-bifenthrin inhibits cortisol and aldosterone biosynthesis in human adrenocortical H295R cells via cAMP signaling cascade. *Environ. Toxicol. Pharmacol.* **2022**, *89*, 103784. [[CrossRef](#)] [[PubMed](#)]
42. Kim, K.B.; Anand, S.S.; Kim, H.J.; White, C.A.; Fisher, J.W.; Tornero-Velez, R.; Bruckner, J.V. Age, dose, and time-dependency of plasma and tissue distribution of deltamethrin in immature rats. *Toxicol. Sci.* **2010**, *115*, 354–368. [[CrossRef](#)] [[PubMed](#)]
43. Chi, C.C.; Chou, C.T.; Liang, W.Z.; Jan, C.R. Effect of the pesticide, deltamethrin, on Ca²⁺ signaling and apoptosis in OC2 human oral cancer cells. *Drug. Chem. Toxicol.* **2014**, *37*, 25–31. [[CrossRef](#)] [[PubMed](#)]
44. Kumar, A.; Sasmal, D.; Sharma, N.; Bhaskar, A.; Chandra, S.; Mukhopadhyay, K.; Kumar, M. Deltamethrin, a pyrethroid insecticide, could be a promising candidate as an anticancer agent. *Med. Hypotheses* **2015**, *85*, 145–147. [[CrossRef](#)] [[PubMed](#)]
45. Klumpp, L.; Sezgin, E.C.; Eckert, F.; Huber, S.M. Ion Channels in Brain Metastasis. *Int. J. Mol. Sci.* **2016**, *17*, 1513. [[CrossRef](#)] [[PubMed](#)]
46. Lee, H.H.; Chou, C.T.; Liang, W.Z.; Chen, W.C.; Wang, J.L.; Yeh, J.H.; Kuo, C.C.; Shieh, P.; Kuo, D.H.; Chen, F.A.; et al. Ca²⁺ Movement Induced by Deltamethrin in PC3 Human Prostate Cancer Cells. *Chin. J. Physiol.* **2016**, *59*, 148–155. [[CrossRef](#)] [[PubMed](#)]
47. Sharma, N.; Banerjee, S.; Mazumder, P.M. Evaluation of the mechanism of anticancer activity of deltamethrin in Jurkat-J6 cell line. *Pestic. Biochem. Physiol.* **2018**, *149*, 98–103. [[CrossRef](#)] [[PubMed](#)]
48. Han, B.; Lv, Z.; Zhang, X.; Lv, Y.; Li, S.; Wu, P.; Yang, Q.; Li, J.; Qu, B.; Zhang, Z. Deltamethrin induces liver fibrosis in quails via activation of the TGF-β1/Smad signaling pathway. *Environ. Pollut.* **2020**, *259*, 113870. [[CrossRef](#)]
49. Sontheimer, H.; Black, J.A.; Waxman, S.G. Voltage-gated Na⁺ channels in glia: Properties and possible functions. *Trends Neurosci.* **1996**, *19*, 325–331. [[CrossRef](#)]
50. Rizaner, N.; Onkal, R.; Fraser, S.P.; Pristerá, A.; Okuse, K.; Djamgoz, M.B. Intracellular calcium oscillations in strongly metastatic human breast and prostate cancer cells: Control by voltage-gated sodium channel activity. *Eur. Biophys. J.* **2016**, *45*, 735–748. [[CrossRef](#)]
51. Gumushan Aktas, H.; Akgun, T. Naringenin inhibits prostate cancer metastasis by blocking voltage-gated sodium channels. *Biomed. Pharmacother.* **2018**, *106*, 770–775. [[CrossRef](#)] [[PubMed](#)]
52. Lai, M.C.; Tzeng, R.C.; Huang, C.W.; Wu, S.N. The Novel Direct Modulatory Effects of Perampanel, an Antagonist of AMPA Receptors, on Voltage-Gated Sodium and M-type Potassium Currents. *Biomolecules* **2019**, *9*, 638. [[CrossRef](#)] [[PubMed](#)]
53. Varró, P.; Kovács, M.; Világi, I. The insecticide esfenvalerate modulates neuronal excitability in mammalian central nervous system in vitro. *Toxicol. Lett.* **2017**, *267*, 39–44. [[CrossRef](#)] [[PubMed](#)]
54. Baron, S.; Barrero, R.A.; Black, M.; Bellgard, M.I.; van Dalen, E.M.S.; Fourie, J.; Maritz-Olivier, C. Differentially expressed genes in response to amitraz treatment suggests a proposed model of resistance to amitraz in *R. decoloratus* ticks. *Int. J. Parasitol. Drugs Drug Resist.* **2018**, *8*, 361–371. [[CrossRef](#)]
55. Pitzer, E.M.; Sugimoto, C.; Gudelsky, G.A.; Huff Adams, C.L.; Williams, M.T.; Vorhees, C.V. Deltamethrin Exposure Daily From Postnatal Day 3–20 in Sprague-Dawley Rats Causes Long-term Cognitive and Behavioral Deficits. *Toxicol. Sci.* **2019**, *169*, 511–523. [[CrossRef](#)]
56. Carpenter, J.M.; Brown, K.A.; Diaz, A.N.; Dockman, R.L.; Benbow, R.A.; Harn, D.A.; Norberg, T.; Wagner, J.J.; Filipov, N.M. Delayed treatment with the immunotherapeutic LNFPIII ameliorates multiple neurological deficits in a pesticide-nerve agent prophylactic mouse model of Gulf War Illness. *Neurotoxicol. Teratol.* **2021**, *87*, 107012. [[CrossRef](#)]
57. Cassano, G.; Bellantuono, V.; Ardizzone, C.; Lippe, C. Pyrethroid stimulation of ion transport across frog skin. *Environ. Toxicol. Chem.* **2003**, *22*, 1330–1334. [[CrossRef](#)]

58. Peng, C.-C.; Li, Y.-R. Parameters Identification of Nonlinear Lorenz Chaotic System and its Application to High Precision Model Reference Synchronization. *Res. Sq.* **2021**. [[CrossRef](#)]
59. Cho, H.Y.; Chuang, T.H.; Wu, S.N. Effective Perturbations on the Amplitude and Hysteresis of Erg-Mediated Potassium Current Caused by 1-Octylnonyl 8-[(2-hydroxyethyl)[6-oxo-6(undecyloxy)hexyl]amino]-octanoate (SM-102), a Cationic Lipid. *Biomedicines* **2021**, *9*, 1367. [[CrossRef](#)]